Nigerian Journal of Physics (NJP)
ISSN online: 3027-0936
ISSN print: 1595-0611
DOI: https://doi.org/10.62292/njp.v35i1.2026.469
Volume 35(1), March 2026

Study of Gamma Ray Shielding Characteristics and Exposure Buildup Factor for some Natural Rocks

Abdulkadir Adamu, Aliyu Mohammed Aliyu, Dauda Abubakar, Abubakar Abba Aji, Alameen Mustapha Muhammed and Umar Haruna

Department of Physics, Sa'adu Zungur University, Bauchi State, Nigeria.

*Corresponding Author's Email: officialtaneez@gmail.com Phone: +2348169173215

ABSTRACT

This study assessed the gamma-ray shielding potential and exposure build up factor of Gypsum, kaolin, limestone and granite commonly used as a building material in Northeastern, Nigeria. The elemental composition of the rocks was obtained through Energy dispersive X-ray spectroscopy (EDX) which examines the microstructural and localized area elemental analyses of the four rock samples. Phy-X software was used to determine and evaluate the radiation shielding parameters at energy range of from 0.015 MeV to 15 MeV originating from ^{137}Cs and ^{60}Co sources. The MAC and LAC showed a decreasing pattern as photon energy increased. In the energy interval of 0.1–0.8 MeV, the MAC and LAC values of all studied materials converged, suggesting comparable attenuation characteristics. A significant drop at lower photon energies was also observed, primarily due to the strong inverse relationship between the photoelectric effect and photon energy. Among all materials, kaolin exhibited higher MAC and LAC values, which can be explained by its higher density and the presence of heavy elements like Ba, Ti, and Fe. The study's findings showed that the natural rocks examined had strong cap abilities to block gamma rays indicating their potential use in radiation protection.

Keywords:
Gamma Radiation,
Shielding Material,
Natural Rocks,
Phy-X/PSD,
Exposure Buildup Factor.

INTRODUCTION

Devices that generate artificial ionizing radiation, such as X-rays and ɣ-rays, have been widely adopted in a variety of industrial, medical, and nuclear configurations. This widespread adoption is a direct result of the utilization of technological breakthroughs (Nabil et al., 2024). Nevertheless, prolonged and excessive exposure to such radiation can have adverse effects on health, potentially leading to the development of cancer, as well as symptoms such as vomiting, nausea, and, in severe situations, even mortality. The interaction of high-energy photons with human tissue results in the ionization of water molecules within the tissue. Due to the fact that it causes harm to both the exterior surface and the inside content of DNA, this ionization should be avoided at all costs. Neutrons, γ-rays, and X-rays pose a threat to the environment, as well as to people and animals. For all of these reasons, the pursuit of discovering improved materials for radiation attenuation and shielding is something that a lot of researchers are interested in (El-Rehim et al., 2020).

To decrease the amount of hazardous radiation that workers are exposed to, it is well known that shielding and attenuation materials act as a barrier between the sources of radiation that release radiation and the surrounding area or the workers themselves. When it comes to minimizing or reducing the potentially harmful effects of radiation, one of the fundamental concepts of radiation protection is the selection of appropriate shielding materials (Kaewkhao et al., 2017). This is a fundamental part of the radiation protection process, as the appropriate selection of shielding materials play a critical role in minimizing radiation exposure and ensuring the safety of personal and the surrounding environment, is still the subject of investigations and study inquiries that are currently being carried out. Polymers, natural rocks, rubber, concrete, brick, clays and alloy are among the materials that have been extensively investigated for radiation shielding applications in numerous studies reported in the literature (Akkurt et al., 2004; Mansour et al., 2020; Almatari et al., 2022).

Additionally, there is recent research about using natural raw materials and rocks as a radiation shield. Minerals are one of these natural raw materials such as halloysite (Mansour et al., 2020), barite (Akkurt et al., 2015), magnetite, limonite, hematite (Oto et al., 2017) and quartz (Marquez et al., 2021). Hence, the importance of applied mineralogy, as a branch of geology, appears in some recent studies to characterize the application of different minerals and rocks as barriers to attenuate the radiation or restrict the migration and dispassion radioactive wastes generated from nuclear facilities by acting as physical barrier that attenuate ionizing radiation and limit radionuclide transport through the absorption, immobilization and containment within their mineral structures. According to global initiatives for sustainability, the use of minerals and rocks, in their native status, in radiation attenuation is preferred over concrete, which remains the most commonly used materials for mitigating the effect of radiation leakage do to the lower environmental impact and reduced energy requirement associated with their extraction and processing (Hemid et al., 2021).

The amount of silica in these rocks is somewhat moderate, and the amount of alkali metals they contain is relatively low (Bonewitz et al., 2012). Since these natural materials have been used as building materials since the beginning of human civilization, it is essential to study their attenuation properties. These rocks are characterized by relatively high density (Average value of about 2.75g cm^{-3}), mechanical hardness durability, and low cost, making them effective and practical materials for radiation shielding due to their ability to attenuate ionizing radiation rather than mere convenience of use. Moreover, various types of high-resistance anti-radiation concrete can be synthesized by using granites or granite-like rock waste as fine or coarse aggregates of anti-concrete mix (El-Nahal et al., 2021). The melting point of igneous rocks is high enough to bear the thermal effect of being exposed to a high dose of ionizing radiation, which ranges from 1215 to 1260 °C at ambient pressure. Therefore, the physical properties of the materials that were investigated are very suitable for operation in harsh radiological environments, such as those found in nuclear reactors. Furthermore, these igneous rocks that are readily available in the environment have the potential to be effective radiation-shielding material candidates. They also represent an environmentally friendly and convenient alternative to conventional radiation-shielding materials such as lead, tungsten, and steel, as well as the extraction, mining, and manufacturing processes that have significant negative effects on the environment and human health (Elsafi et al., 2021).

By measuring the linear/mass attenuation factors theoretically and experimentally, this study aims to determine the shielding properties against radiation of the selected types of rocks (diorite, kaolin, limestone and granite). Following this, the attenuation parameters, such as the half value layer and radiation protection efficiency, will be deduced. This will allow for the evaluation of the effectiveness of using these materials as radiation protection materials. This research aims to investigate the nuclear radiation shielding properties of selected rock types, namely Gypsum, Kaolin, Limestone, and Granite.

MATERIALS AND METHODS

The research determined gamma radiation and neutron shielding properties of various selected types of rocks (Gypsum, kaolin, limestone and granite). The samples elemental composition was determined using Energy Dispersive X-ray spectroscopy (EDX). The shielding parameters such as mass attenuation coefficient (MAC), linear attenuation coefficient (LAC), mean free path (MFP) the exposure buildup factor (EBF) and equivalent atomic number (Zeq) were determined using Phy-X/PSD simulation software.

Sample Collection

Four different types of rocks (Gypsum, kaolin, limestone and granite) were obtained with the aid of local suppliers from the areas of Bauchi and Gombe state as shown in the fig 3.1. These rocks are igneous rocks which crystallize and solidify from magma in deep levels from the earth crust. So, they are very hard, massive, and have high specific gravity. Depending on this nature, they have variable uses such as crushed stones for road building, construction materials, paving, countertops, tile floors, in addition they were used in construction of ancient pharaonic statues. The investigated rocks, with typical chemical compositions shown in Table 1, were handled in the form of 3 mm in thickness. They were cut in the form of 70 × 70 mm squares to fit the supporting frame in front of the experimental work.

Figure 1: Samples Images for Investigated Rocks Samples

Sample Preparation

The selected materials were collected in plastic polyethylene bags, weighed, packed, and transported to the laboratories at the Umaru Musa Yardua University, Kastina for preparation and analysis. The collected samples were oven dried at 105 °C for 24 h in order to remove moisture contents and then allowed to cool down to room temperature and later crushed, grounded and then sieved for homogeneity using 500 µm and 250 µm mesh.

Table 1: Chemical Composition and Density of the Investigated Rock Samples

Samples	Composition by weight %													Density (g/cm^3)
	K	Ca	H	Mg	Ba	Na	Si	Ti	Fe	O	Mn	Al	C	
Granite	1.32	4.38	BDL	4.48	BDL	1.42	37.96	BDL	9.74	BDL	BDL	12.64	28.06	2.57
Gypsum	0.08	96.42	BDL	0.32	BDL	0.04	0.35	BDL	2.62	BDL	0.04	0.13	BDL	2.43
Kaolin	4.29	11.82	BDL	1.74	0.12	1.47	55.07	0.57	2.65	BDL	0.06	22.21	BDL	2.72
Limestone	3.09	12.52	0.89	1.83	BDL	1.97	21.31	0.32	3.64	53.92	0.21	0.30	BDL	2.15

Measurement of Elemental Compositions using Energy Dispersive X-ray Spectroscopy (EDX)

EDX divides the following investigation into two main parts. The first section examines the microstructural and localized area elemental analyses of the four rock samples. The EDX works in conjunction with a scanning electron microscope, where the sample is carefully prepared, often by cutting it into small pieces or grinding it to prepare it for analysis, and more than one area of the sample is analyzed. Electron microscopes are used shine a a beam of electrons on the sample, this beam electrons to be emitted from the causes elements in the sample. The energy from the emitted electrons is collected in the EDX system.

Each element has a specific energy for the emitted electrons, allowing, the elements in the sample to be identified. EDX produces a spectrum that shows peaks representing the different elements.

These peaks are analyzed to determine the active elements and their amounts.

Measurement of density of the samples Furthermore, the mass density of the prepared samples was determined from the calculated mass of each sample using a digital beam balance, and the volume of each sample was calculated from the dimensions of the samples and the density was obtained using Eq 1

$$\rho = {}^{m}/_{V} \quad (1)$$

where:

ρ is Density (g cm^{-3}), m is the mass (g) and V is the volume (cm^3)

Radiation Shielding Simulation

The radiation shielding parameters of the four different types of rocks (diorite, kaolin, limestone and granite) will be determined theoretically using user friendly online Phy-X/PSD software developed by Sakar *et al*. 2020. The shielding parameters investigated include the mass attenuation coefficient (MAC), linear attenuation coefficient (LAC), mean free path (MFP), half-value layer (HVL), equivalent atomic number (Zeq), and exposure buildup factor (EBF). Calculations were performed over a photon energy range of 0.015–15 MeV, corresponding to energies emitted by common gamma-ray sources such as ^{137}Cs and ^{60}Co.

PHY-X/PSD Software

The simulation process using Phy-X/PSD was carried out in three stages:

Stage 1: Material Definition

The chemical compositions of the rock samples, obtained from EDX analysis, were entered into the software using weight fraction representation. The experimentally determined mass density of each sample was also provided, as it is required for the computation of shielding parameters. Each material was assigned an identifying label to organize the calculation outputs.

Stage 2: Selection of Photon Energies

Photon energies ranging from 15 KeV to 15 MeV were selected for the simulations. These energies are relevant for radiation shielding studies and are available within the Phy-X/PSD database, which includes several standard radioactive sources and characteristic X-ray energies.

Stage: 3 Selection of Shielding Parameters

The required shielding parameters—MAC, LAC, MFP, HVL, Zeq, and EBF—were selected for computation. After successful execution of the simulations, the results were exported for analysis and graphical representation.

RESULTS AND DISCUSSION

The gamma-ray shielding properties of gypsum, kaolin, limestone, and granite were evaluated theoretically using Phy-X/PSD simulation software. Shielding parameters including mass attenuation coefficient (MAC), linear attenuation coefficient (LAC), mean free path (MFP), equivalent atomic number (Zeq), and exposure buildup factor (EBF) were determined for photon energies ranging from 0.015 MeV to 15 MeV.

Mass Attenuation (MAC) and Linear Attenuation Coefficient (LAC)

The variation of MAC and LAC with photon energy for the investigated rock samples is presented in Figures 2 and 3, respectively. For all samples, both MAC and LAC exhibited a decreasing trend with increasing photon energy. This behavior is attributed to the reduction in photoelectric absorption probability and Compton scattering dominance as photon energy increases.

At low photon energies (< 0.1 MeV), a sharp decrease in attenuation coefficients was observed. This is due to the strong inverse dependence of the photoelectric effect on photon energy, which varies approximately as . In the intermediate energy range of 0.1–0.8 MeV, the MAC and LAC values for all samples converged, indicating comparable attenuation behavior among the materials. (Alalawi, et al., 2023).

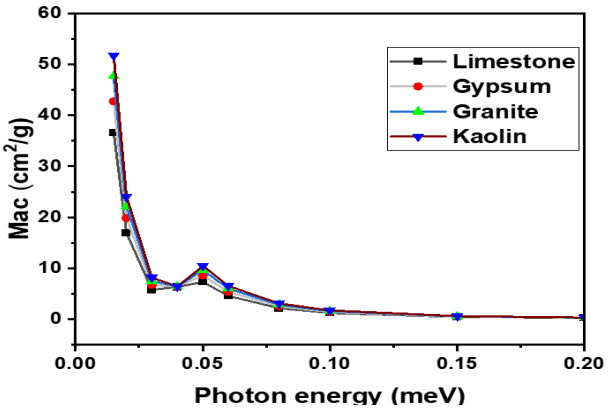

Figure 2: Variation of MAC of the Rock Samples with Photon Energy by (Alalawi, et al., 2023)

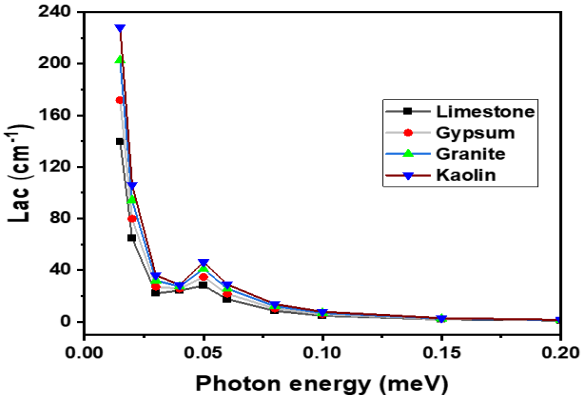

Figure 3: Variation of LAC of the Rock Samples with Photon Energy (Sayyed, M. I., 2018) and (Almatari, et al., 2022)

Among the investigated samples, kaolin consistently exhibited the highest MAC and LAC values across the entire energy range. This enhanced attenuation performance can be attributed to its relatively higher density and the presence of high atomic number elements such as Ba, Ti, and Fe. Since attenuation coefficients depend strongly on material density and atomic number, the composition of kaolin significantly enhances its gamma-ray interaction probability. by (Sayyed, M. I., 2018) and (Almatari, et al., 2022).

Mean Free Path (MFP)

The Fig 4 indicates that MFP values increase with rising photon energy. At low energy levels (< 0.8 MeV), all samples exhibit nearly identical MFP values, likely due to their similar chemical compositions, aligning with (Al-Singh et al., 2014) findings. As photon energy rises, MFP also increase, reaching their peak values at the highest energies. Above 2.0 MeV, a slight increase in MFP is observed, which is likely attributed to the influence of high-Z elements and the onset of pair production, as discussed by Al-Buriahi et al. Furthermore, the samples consistently show similar values at specific gamma

energies due to comparable high-Z elemental compositions. Materials with lower MFP offer better shielding efficiency, consistent with (Almousa et al., 2024)'s findings. Overall, MFP are affected by the material's composition, density, and photon energy. Among the materials studied, Kaolin displayed the lowest MFP values, indicating its superior gamma shielding compared to the others.

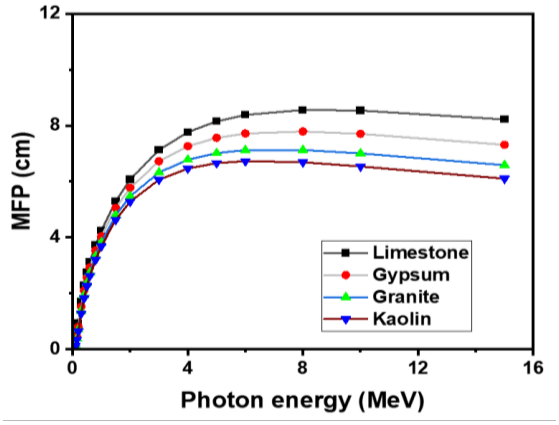

Figure 4: Variation of MFP of the Rock Samples with Photon Energy (Almousa et al., 2024)'s

Equivalent Atomic Number (Z_{eq})

The equivalent atomic number (Z_{eq}) is a parameter which measure how incident radiation interacts with multi element material, greater value of Z_{eq} signifies a better shield. Fig. 5 illustrates the variation of Z_{eq} against the incident photon energy. The Z_{eq} values initially, increases from 15 to 60 MeV and then decreases as the energy as photon energy rises above 60 MeV. Limestone has the least Z_{eq} value of 42.81, while kaolin has the highest with value of 57.68 at 60 MeV. The trend implies that high content of Ba, Ti, Fe and the high density in kaolin helps to increase the average atomic number of compound mixture and eventually improve the shielding properties of glasses.

It was observed that the values of Zeq for all samples were higher at the lower energy region, this is primarily due to the photoelectric interaction which directly depends on the atomic number, Z^4, and the photon energy as, $E^{-3.5}$, for any absorber. At the intermediate photon energy, the Zeq decreases slowly with the increase of incident photon energy and becomes almost independent of the photon energy for all the samples which agrees with the work of (Al-Saleh., 2024). As the photon energy increases above 3.0 MeV, the value of Zeq showed a little increment and this behavior could be due to the high Z-element dependency and the dominance of pair production at higher energy region. At low energy region, the highest value of Zeq was observed for Kaolin and the minimum value was observed for Limestone sample, this indicated that Zeq *is* linearly related to the Z-elements in the sample as earlier reported by (Abbas, et al., 2022). Generally, it was observed that the Zeq values of the samples decreased with increasing incident photon energies.

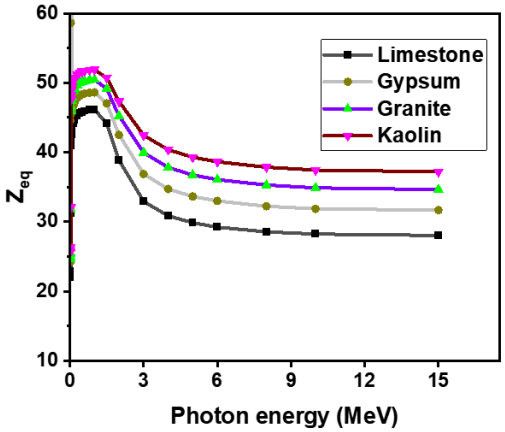

Figure 5: Variation of Zeq of the Rock Samples with Photon Energy (Al-Saleh., 2024)

Exposure Buildup Factor (EBF)

In this research, the EBF parameter was calculated using Phy-X/PSD to thoroughly assess how well the rock samples protect against radiation. Key contributors to the buildup factor included the effective atomic number, the energy of the incident gamma rays, the depth of their penetration, and the specific chemical components of the material.

Table 2: G-P Fitting Coefficients for the Limestone Rock Sample, Corresponding to the EBF Parameters

Energy (MeV)	Zeq	G-P parameters for EBF				
		A	B	C	Xk	D
1.50E-02	11.19	0.221	1.049	0.383	12.014	-0.118
2.00E-02	11.35	0.200	1.109	0.413	13.828	-0.106
3.00E-02	11.56	0.183	1.331	0.462	14.475	-0.098
4.00E-02	11.71	0.131	1.663	0.587	15.521	-0.068
5.00E-02	15.07	0.163	1.527	0.518	14.684	-0.091
6.00E-02	15.40	0.126	1.704	0.610	14.719	-0.069
8.00E-02	15.89	0.075	1.990	0.762	14.707	-0.045
1.00E-01	16.25	0.052	2.233	0.861	13.190	-0.044
1.50E-01	16.85	-0.006	2.388	1.092	12.951	-0.022
2.00E-01	17.23	-0.028	2.404	1.210	11.653	-0.017
3.00E-01	17.70	-0.049	2.314	1.319	8.843	-0.010
4.00E-01	18.00	-0.054	2.234	1.342	8.273	-0.009
5.00E-01	18.17	-0.065	2.141	1.375	22.018	0.017
6.00E-01	18.29	-0.065	2.083	1.364	18.715	0.014
8.00E-01	18.40	-0.063	1.988	1.336	16.683	0.015
1.00E+00	18.43	-0.058	1.920	1.299	15.943	0.016
1.50E+00	12.76	-0.048	1.858	1.231	15.656	0.017
2.00E+00	10.45	-0.034	1.802	1.156	14.585	0.012
3.00E+00	9.92	-0.011	1.693	1.055	11.250	0.001
4.00E+00	9.81	0.005	1.612	0.991	15.608	-0.008
5.00E+00	9.75	0.016	1.542	0.953	14.905	-0.017
6.00E+00	9.73	0.029	1.498	0.915	13.025	-0.024
8.00E+00	9.70	0.033	1.410	0.898	13.043	-0.023
1.00E+01	9.68	0.041	1.351	0.874	13.511	-0.030
1.50E+01	9.67	0.058	1.264	0.831	14.625	-0.049

Tables 2 through 5 present the equivalent atomic numbers (Zeq) and the GP fitting parameters of the EBF for the four rock samples, spanning a broad gamma-ray energy range from 0.015 to 15 MeV and penetration depths from 0.5 to 40 mfp. Prior research indicates that materials with lower EBF values demonstrate superior shielding performance (Sayyed, M. I., 2018).

Table 3: G-P Fitting Coefficients for the Gypsum Rock Sample, Corresponding to the EBF Parameters

Energy (MeV)	Zeq	G-P parameters for EBF				
		a	B	C	Xk	D
1.50E-02	11.62	0.215	1.043	0.393	12.717	-0.126
2.00E-02	11.80	0.184	1.092	0.431	14.189	-0.095
3.00E-02	12.06	0.190	1.284	0.447	14.428	-0.102
4.00E-02	12.26	0.149	1.581	0.543	15.066	-0.079
5.00E-02	16.79	0.187	1.388	0.465	14.455	-0.105
6.00E-02	17.19	0.157	1.526	0.535	14.459	-0.088
8.00E-02	17.79	0.107	1.760	0.666	14.442	-0.061
1.00E-01	18.22	0.063	1.928	0.801	14.470	-0.043
1.50E-01	18.92	0.010	2.154	1.008	13.677	-0.022
2.00E-01	19.36	-0.018	2.213	1.148	12.155	-0.016
3.00E-01	19.92	-0.039	2.208	1.259	10.251	-0.011
4.00E-01	20.24	-0.046	2.164	1.294	9.804	-0.009
5.00E-01	20.45	-0.047	2.114	1.299	8.679	-0.011
6.00E-01	20.58	-0.057	2.046	1.324	21.947	0.012

Energy (MeV)	Zeq	G-P parameters for EBF				
		a	B	C	Xk	D
8.00E-01	20.72	-0.057	1.955	1.310	17.497	0.013
1.00E+00	20.75	-0.055	1.895	1.284	17.454	0.016
1.50E+00	14.64	-0.047	1.837	1.227	15.275	0.016
2.00E+00	11.23	-0.034	1.793	1.154	14.827	0.012
3.00E+00	10.40	-0.011	1.689	1.055	10.896	0.001
4.00E+00	10.22	0.006	1.610	0.992	14.630	-0.008
5.00E+00	10.13	0.016	1.540	0.954	14.999	-0.018
6.00E+00	10.09	0.029	1.497	0.915	12.533	-0.024
8.00E+00	10.04	0.033	1.409	0.899	13.178	-0.024
1.00E+01	10.02	0.042	1.350	0.875	13.425	-0.031
1.50E+01	10.00	0.060	1.264	0.829	14.553	-0.051

The dependency of EBF on photon energy at constant penetration depths (15 mfp) for the different rock sample is shown in Fig. 6 For energies below 0.1 MeV, the EBF remains consistently low across all Samples. This is attributed to the photoelectric effect, which dominates at such low energies and has a highly energy-sensitive cross section that decreases sharply (as $E^{-3.5}$), causing efficient photon absorption. At higher energies, pair production becomes the prevailing interaction, with its cross section also decreasing with energy (E^{-2}), again promoting high photon absorption. A notable rise in EBF is detected near 0.1 MeV, with a gradual increase as energy rises further, mainly due to the increased frequency of Compton scattering events, continuing up to about 5 MeV (Al-Buriahi et al., 2019).

Table 4: G-P Fitting Coefficients for the Granite Rock Sample, Corresponding to the EBF Parameters

Energy (MeV)	Zeq	G-P parameters for EBF				
		a	B	C	Xk	D
1.50E-02	11.99	0.211	1.037	0.401	13.316	-0.133
2.00E-02	12.22	0.188	1.081	0.426	14.219	-0.098
3.00E-02	12.53	0.194	1.253	0.435	14.766	-0.103
4.00E-02	12.75	0.160	1.514	0.516	14.876	-0.086
5.00E-02	18.16	0.204	1.306	0.429	14.225	-0.117
6.00E-02	18.61	0.174	1.417	0.493	14.356	-0.097
8.00E-02	19.27	0.133	1.622	0.599	14.328	-0.076
1.00E-01	19.74	0.089	1.783	0.720	14.308	-0.056
1.50E-01	20.51	0.029	2.023	0.929	13.732	-0.030
2.00E-01	21.01	-0.003	2.112	1.079	12.702	-0.022
3.00E-01	21.60	-0.030	2.136	1.210	10.729	-0.013
4.00E-01	21.97	-0.040	2.108	1.259	10.104	-0.011
5.00E-01	22.19	-0.044	2.064	1.279	8.564	-0.009
6.00E-01	22.33	-0.051	2.011	1.297	17.149	0.005
8.00E-01	22.48	-0.050	1.938	1.282	14.069	0.004
1.00E+00	22.51	-0.052	1.876	1.271	18.190	0.015
1.50E+00	16.31	-0.044	1.829	1.214	16.136	0.013
2.00E+00	11.99	-0.033	1.787	1.155	16.094	0.011
3.00E+00	10.87	-0.011	1.685	1.056	10.562	0.001
4.00E+00	10.62	0.006	1.608	0.992	13.703	-0.009
5.00E+00	10.51	0.016	1.538	0.955	15.089	-0.019
6.00E+00	10.46	0.030	1.496	0.914	12.059	-0.024
8.00E+00	10.39	0.033	1.408	0.900	13.310	-0.025
1.00E+01	10.36	0.042	1.349	0.875	13.341	-0.032
1.50E+01	10.34	0.061	1.263	0.827	14.482	-0.053

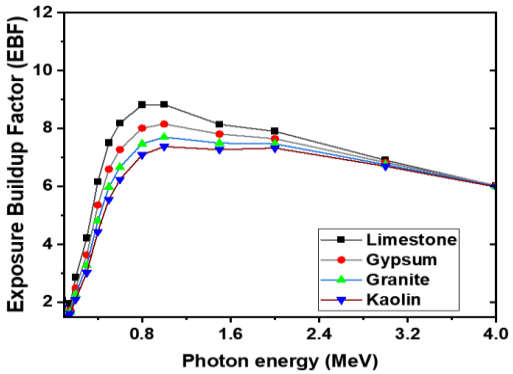

Figure 6: Variation of Exposure Buildup Factors with Photon Energy at 15 mfp (Al-Buriahi et al., 2019)

The exposure buildup factor was evaluated to assess the contribution of scattered radiation to total exposure. Figures and Tables 2–5 present the G–P fitting parameters and EBF variations for penetration depths up to 40 mean free paths.

At low photon energies (< 0.1 MeV), the EBF values were minimal for all samples due to strong photoelectric absorption. As photon energy increased, the EBF values rose sharply and reached maximum values in the intermediate energy region, where Compton scattering dominates. At higher photon energies (> 5 MeV), the EBF values decreased due to increased pair production probability.

Limestone, which has the lowest equivalent atomic number, exhibited the highest EBF values, while kaolin exhibited the lowest EBF values. This inverse relationship between Zeq and EBF indicates that materials with higher effective atomic numbers are more effective in suppressing scattered radiation. Consequently, kaolin demonstrated the most favorable EBF behavior among the investigated samples.

Table 5: G-P Fitting Coefficients for the Kaolin Rock Sample, Corresponding to the EBF Parameters

Energy (MeV)	Zeq	G-P parameters for EBF				
		a	B	C	Xk	D
1.50E-02	12.53	0.208	1.033	0.397	14.501	-0.136
2.00E-02	12.78	0.211	1.071	0.396	13.921	-0.114
3.00E-02	13.14	0.201	1.217	0.418	14.945	-0.106
4.00E-02	13.40	0.175	1.441	0.485	14.596	-0.096
5.00E-02	19.83	0.214	1.233	0.405	14.150	-0.119
6.00E-02	20.33	0.193	1.323	0.453	14.245	-0.111
8.00E-02	21.07	0.150	1.505	0.553	14.376	-0.084
1.00E-01	21.59	0.108	1.652	0.664	14.245	-0.064
1.50E-01	22.43	0.048	1.886	0.859	13.878	-0.037
2.00E-01	22.97	0.012	1.998	1.009	12.923	-0.027
3.00E-01	23.61	-0.020	2.058	1.155	11.271	-0.016
4.00E-01	24.01	-0.033	2.047	1.221	10.428	-0.012
5.00E-01	24.24	-0.041	2.010	1.257	8.439	-0.008
6.00E-01	24.39	-0.045	1.974	1.268	11.952	-0.004
8.00E-01	24.55	-0.043	1.918	1.252	10.347	-0.005
1.00E+00	24.59	-0.050	1.854	1.258	18.987	0.014
1.50E+00	18.49	-0.044	1.809	1.213	15.764	0.013
2.00E+00	13.09	-0.032	1.780	1.153	15.248	0.009
3.00E+00	11.55	-0.012	1.678	1.061	13.861	-0.001
4.00E+00	11.21	0.006	1.604	0.993	12.895	-0.009
5.00E+00	11.07	0.017	1.536	0.955	14.832	-0.021
6.00E+00	10.99	0.031	1.494	0.914	11.394	-0.025
8.00E+00	10.90	0.033	1.406	0.902	13.494	-0.026
1.00E+01	10.85	0.043	1.347	0.876	13.223	-0.033
1.50E+01	10.83	0.063	1.263	0.824	14.384	-0.055

Variations in EBF are primarily caused by differences in Ba, Ti and Fe across the samples, highlighting the role of elemental composition in radiation shielding. The high content of Ba, Ti, Fe and the high density in kaolin leads to a reduction in EBF. Kaolin appears as best gamma ray shielding glass due to higher values for Z_{eq} and lower values of EBF. Previous findings suggest that the shielding efficiency of a material improves as its EBF decreases (Al-Singh et al., 2014).

CONCLUSION

The gamma shielding behavior of four different types of rocks (Gypsum, kaolin, limestone and granite) were determined using Phy-X/PSD software. Theoretical calculations of the Mass Attenuation Coefficient (MAC) and Linear Attenuation Coefficient (LAC) were carried out across the energy range of 0.015 MeV to 15 MeV. Both MAC and LAC showed a decreasing pattern as photon energy increased. In the energy interval of 0.1–0.8 MeV, the MAC and LAC values of all studied materials converged, suggesting comparable attenuation characteristics. A significant drop at lower photon energies was also observed, primarily due to the strong inverse relationship between the photoelectric effect and photon energy. Among all materials, kaolin exhibited higher MAC and LAC values, which can be explained by its higher density and the presence of heavy elements like Ba, Ti, and Fe. The attenuation coefficients are largely influenced by photon energy, atomic number, and material density, which explains the enhanced values seen in kaolin.

The results indicated that limestone, with the lowest equivalent atomic number (Zeq), exhibited the highest EBF values. In contrast, kaolin, which had the highest Zeq, showed the lowest EBF values. This inverse correlation suggests that as Zeq increases, EBF decreases. The EBF was found to be lowest at both low and high photon energies, with maximum values occurring at intermediate energies. These variations are mainly due to differences in the elemental composition particularly the presence of Ba, Ti, and Fe across the samples. Kaolin's high concentrations of these elements, along with its higher density, contributed to the reduction in EBF. As a result, kaolin is identified as the most effective material for gamma-ray shielding, owing to its high Zeq and low EBF values.

REFERENCES

Abbas, M. I., Alahmadi, A. H., Elsafi, M., Alqahtani, S. A., Yasmin, S., Sayyed, M. I. and El-Khatib, A. M. (2022). Effect of kaolin clay and ZnO nanoparticles on the radiation shielding properties of epoxy resin composites. Polymers, 14(22), 4801.

AbuAlRoos, N. J., Azman, M. N., Amin, N. A. B. and Zainon, R. (2020). Tungsten-based material as promising new lead-free gamma radiation shielding material in nuclear medicine. Physics in Medicine, 78, 48–57.

Akkurt, I., Kilincarslan, S. and Basyigit, C. (2004). The photon attenuation coefficients of barite, marble and limra. Annals of Nuclear Energy, 31(5), 577–582.

Al-BuriahI, M. S. and Tonguc, B. T. (2019). Study on gamma-ray buildup factors of bismuth borate glasses. Applied Physics A, 125(7), 482.

Al-BuriahI, M. S., Sayyed, M. I. and Kurudirek, M. (2021). Dense and environment-friendly bismuth barium telluroborate glasses for nuclear protection applications. Progress in Nuclear Energy, 137, 103763.

Almatari, M., Koraim, Y., Saleh, I. H., Sayyed, M. I., Khandaker, M. U. and Elsafi, M. (2022). Investigation of the photon shielding capability of kaolin clay added with micro and nanoparticles of Bi_2O_3. Radiation Physics and Chemistry, 200, 110191.

Almousa, N., Issa, S. A., Tekin, H. O., Rammah, Y. S., Mostafa, A. M. A., Baykal, D. S. and Zakaly, H. M. (2024). Enhancing radiation shielding transmission factors and mechanical robustness of borosilicate glasses through Bi_2O_3 modification. Radiation Physics and Chemistry, 220, 111683.

Al-Saleh, W. M., Elsafi, M., Almutairi, H. M., Nabil, I. M. and El-Nahal, M. A. (2024). A comprehensive study of the shielding ability from ionizing radiation of different mortars using iron filings and bismuth oxide. Scientific Reports, 14, 10014.

Bonewitz, R. (2012). Rocks and Minerals. DK Publishing, London.

El-Nahal, M. A., Elsafi, M., Al-Saleh, W. M. and Sayyed, M. I. (2021). Understanding the effect of introducing micro- and nanoparticle bismuth oxide on the gamma-ray shielding performance of concrete. Materials, 14, 6487.

Elsafi, M., Sayyed, M. I., Al-Hadeethi, Y. and Koraim, Y. (2021). The potentials of Egyptian and Indian granites for protection against ionizing radiation. Materials, 14, 3928.

Garba, N. N., Ahmed, A., Muhammad, S. and Lawal, M. (2023). Evaluation of radiological risk associated with local building materials commonly used in Northwestern Nigeria. Heliyon, 9, e15791.

Günoğlu, K., Akkurt, I. and Sayyed, M. I. (2024). Radiation shielding properties of some igneous rocks in Isparta province at different gamma energies. Journal of Radiation Research and Applied Sciences, 17, 100796.

Hemid, E. M., Farkas, C. and Szalai, Z. (2021). Effect of groundwater fluctuation, construction and retaining systems on slope stability. Open Geosciences, 13, 1139–1157.

Kaewkhao, J., Laopaiboon, R., Chewpraditkul, W. and Bootjomchai, C. (2017). Monte Carlo design and experiments on neutron shielding performances of Bi_2O_3–ZnO–B_2O_3 glass systems. Glass Physics and Chemistry, 43, 560–563.

Mansour, A., Sayyed, M. I., El-Sayed, A. A. and Mahmoud, K. A. (2020). Modified halloysite minerals for radiation shielding purposes. Journal of Radiation Research and Applied Sciences, 13(1), 94–101.

Marquez-Mata, C. A., Sayyed, M. I., Khandaker, M. U. and Elsafi, M. (2021). Shielding features of seven types of natural quartz. Applied Radiation and Isotopes, 167, 109450.

Masoud, M. A., Sayyed, M. I., Al-Hadeethi, Y. and Koraim, Y. (2022). Radiation shielding features of heavy minerals in their native status. Sustainability, 14, 16225.

Nabil, I. M., El-Samrah, M. G., Sayed, A. F. E., Shazly, A. and Omar, A. (2024). Radionuclide distribution and radiation hazards assessment of black sand separation plant minerals. Scientific Reports, 14, 5241.

Obaid, S. S., Sayyed, M. I., Gaikwad, D. K. and Pawar, P. P. (2018). Attenuation coefficients and exposure buildup factor of some rocks for gamma-ray shielding applications. Radiation Physics and Chemistry, 148, 86–94.

Oto, B., Akkurt, I., Altinsoy, N. and Buyuk, B. (2015). Investigation of gamma radiation shielding properties of various ores. Progress in Nuclear Energy, 85, 391–403.

Sayyed, M. I. (2018). Investigation of radiation shielding parameters for selected glass systems. Radiation Physics and Chemistry, 150, 120–124.

Singh, V. P., Badiger, N. M., Chanthima, N. and Kaewkhao, J. (2014). Evaluation of gamma-ray exposure buildup factors and neutron shielding for bismuth borosilicate glasses. Radiation Physics and Chemistry, 98, 14–21.

Waly, E.-S. A., Fusco, M. A. and Bourham, M. A. (2016). Gamma-ray mass attenuation coefficients and half-value layer factors of oxide glass shielding materials. Annals of Nuclear Energy, 96, 26–30.